CDF/DOC/TRIGGER/CDFR/xxxx
Version 1.0 – September 14, 2005

Studies of Level 1 Barrel Pointer Performance

Gene Flanagan, Matthew Jones
Purdue University

Jonathan Lewis
Fermilab

1 Introduction

The availability of stereo tracking information from the new SLAM modules makes it possible to extrapolate tracks back to the silicon detector in the Level 1 trigger. This extrapolation provides a way to determine which SVX half-barrels are unlikely to contain hits associated with a track. It may be possible to reduce the average SVT processing time by dropping combinations of XFT tracks and SVX hits in unassociated half-barrels from the list of candidates processed by the track fitter, thus reducing the level 2 processing time on some fraction of events. The studies described here attempt to quantify the benefits of using the level 1 stereo tracking information in this way.

2 Simulation of the XFT Upgrade

The studies described here that are performed on data use the axial tracks identified by the existing XFT system and associates stereo information with them by emulating the hardware components that are currently under development using `XFTSim`[1]. Specifically, the emulation of the stereo finder module[2] provides a list of stereo pixels and the emulation of the SLAM module provides a list of roads associated with the track.

2.1 Stereo finder masks

This section needs to summarize how the stereo finder masks were generated and a discussion of whether the approach used is appropriate for what we need. We probably need input from Greg Veramendi.

The XFT stereo track finding system finds track segments on superlayers 3,5 and 7. These superlayers contain 240,336 and 432 cells respectively, each with 12 wires. Hits on the 12 wires in a superlayer are classified into 6 time bins. The combination of 6 times bins for each of the 12 wires in a given track segment is a mask. The wires hit are not necessarily in the same cell. This relative cell location varies from -2 to +2 for masks going down to P_T of 1.5 GeV. When a mask is found, a pixel is set corresponding to the phi and slope of the mask. There may be hundreds of masks that set the same pixel, depending on how finely the pixels are segmented.

In order to generate the masks, tracks with random curvature are produced with $1.5 < P_T < 1000$ GeV. These tracks are extrapolated through the COT geometry description with a drift time model, and the timing of the hits on each wire is recorded. This was done using `cdfsoft2 4.6.2` (this produces the minimal set of masks, unlike `cdfsoft2 5.X.X`).

Further details about mask generation can be found in [4].

2.2 SLAM roads

This section needs to summarize how the SLAM roads were generated. Are they high efficiency but low purity? Could they be generated in a different way that would reduce the number of SLAM matches while still having high efficiency? Or maybe they are fine the way they are. It would be useful to quantify some of these questions.

The $z0$ and $Cot(\theta)$ values associated with each SLAM road were determined from random tracks. For each track it was determined which stereo pixels would have been set and therefore which SLAM road the track would have fired. The $z0$ and $Cot(\theta)$ for each SLAM road are the average values taken over all the tracks that match to that road. (*need to double check with kevin on this*)

3 Resolution and Efficiency

The resolution of the SLAM roads is studied using axial XFT tracks matched to a parent COT track. The criteria used to perform this matching are as follows:

- Track has $p_T > 1.4$ GeV/c
- The track is a COT track, or is derived from a COT track
- $|\Delta\phi_6| < 5\sigma_{\Delta\phi_6}$
- $|\Delta 1/p_T| < 5\sigma_{\Delta 1/p_T}$

where $\sigma_{\Delta\phi_6} = 1.3$ mrad and $\sigma_{\Delta 1/p_T} = 0.016$ GeV^{-1}. XFT tracks that are matched to COT tracks in this way are associated with stereo segments using the SLAM algorithm which also provides a list of roads with which the combination of axial XFT track and stereo segements is consistent.

The efficiency with which stereo segments are associated with axial XFT tracks using the SLAM algorithm is evaluated by comparing the number of axial XFT tracks matched with an offline COT track with the number of these that are also associated with stereo segments by the SLAM algorithm. The efficiency as a function of the XFT p_T bin is shown in Figure 1 for 1-track Monte Carlo, tracks from the `blpc0d` dataset and tracks from test run x.

Figure 1: SLAM efficiency as a function of XFT p_T bin for tracks in 1-track Monte Carlo (a), in the `blpc0d` dataset (b) and in run x (c).

Each road identified by the SLAM algorithm has associated with it an estimate of z_0 and $\cot\theta$. The resolution with which these r-z track parameters are determined is evaluated by comparing their values associated with the identified SLAM roads with the parameters of the matched offline tracks. In the studies describe here, we are most concerned with an estimate of z at radius that is characteristic of the silicon detector. Thus, we calculate $z_{Si3} = z_0 + r_{Si3}\cot\theta$, which is the z estimate at the mean radius of layer 3 of the silicon detector, $r_{Si3} = 10.5$ cm. We also calculate $z_8 = z_0 + r_{SL8}\cot\theta$, which is the z estimate evaluated at the mean radius of the outermost superlayer of the COT. These resolutions are shown in Figure 4 for each of the three datasets studied.

4 Barrel-pointer performance

The proposed barrel pointer hardware will determine which half-barrels in the SVX-II might contain hits associated with XFT tracks that were confirmed by the SLAM algorithm. Hits in half-barrels to which no XFT track extrapolates can be removed from the list of track fits performed by the track fitter module and will reduce the time needed to fit all XFT track-SVX hit combinations. These fits are performed in each of the 12 SVX wedges in parallel so the improvement in SVT processing time will only come from the reduction in time of the most occupied SVX wedge.

[See if Jonathan can point you to a diagram of the upgraded SVT system and help you draw in this proposed path for the data from SLAM into the barrel pointer hardware and then into the SVT.]

4.1 Ideal case

The best possible performance that the proposed barrel pointer hardware could provide is evaluated using SVT tracks matched with offline tracks using their ϕ_0 and curvatures by applying the method used by, for example, `LeptonSvtSel`[3]. Figure 2 shows the maximum number of SVX half-barrels containing confirmed SVT tracks of all 12 SVX wedges. In this ideal case, the mean is reduced from exactly 6 to 1.03 in the case of `blpc0d` data recorded at an instantaneous luminosity of z cm^{-2}s^{-1}.

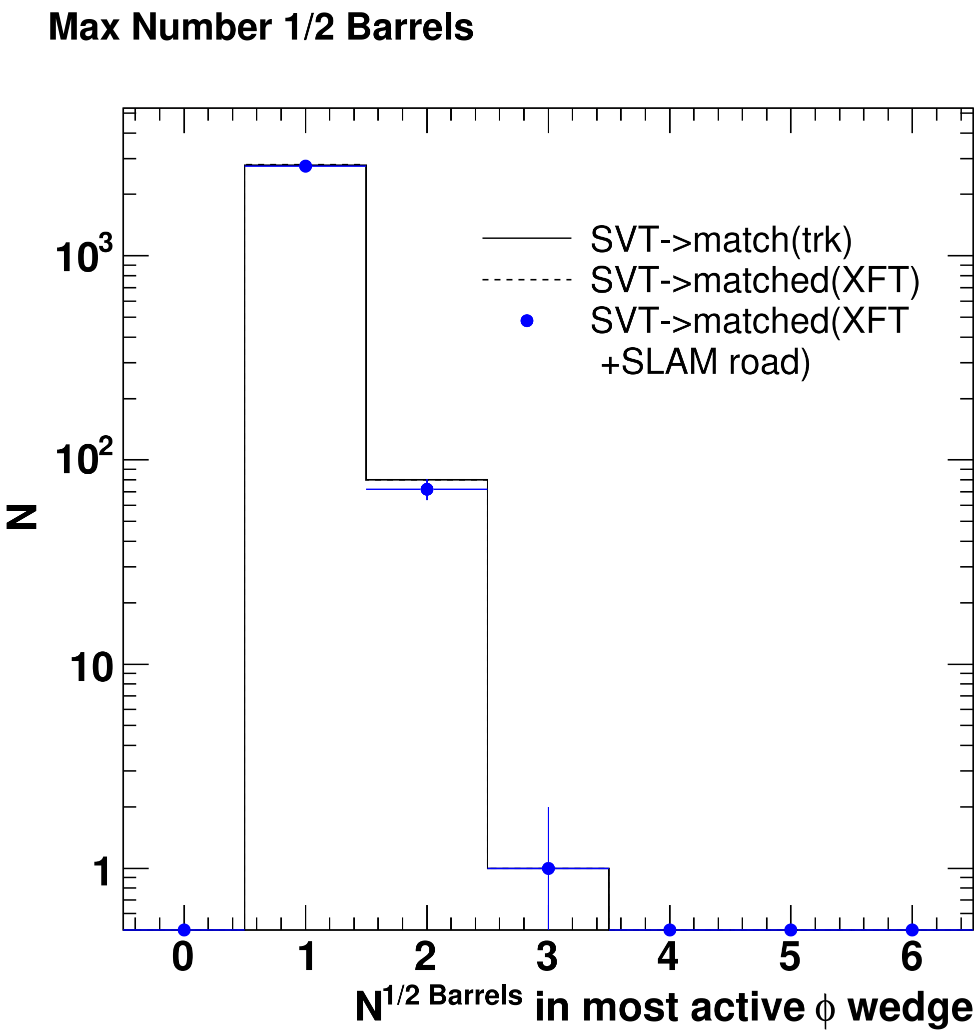

Figure 2: Maximum number of SVX-II half-barrels containing matched SVT tracks in the `blpc0d` data set.

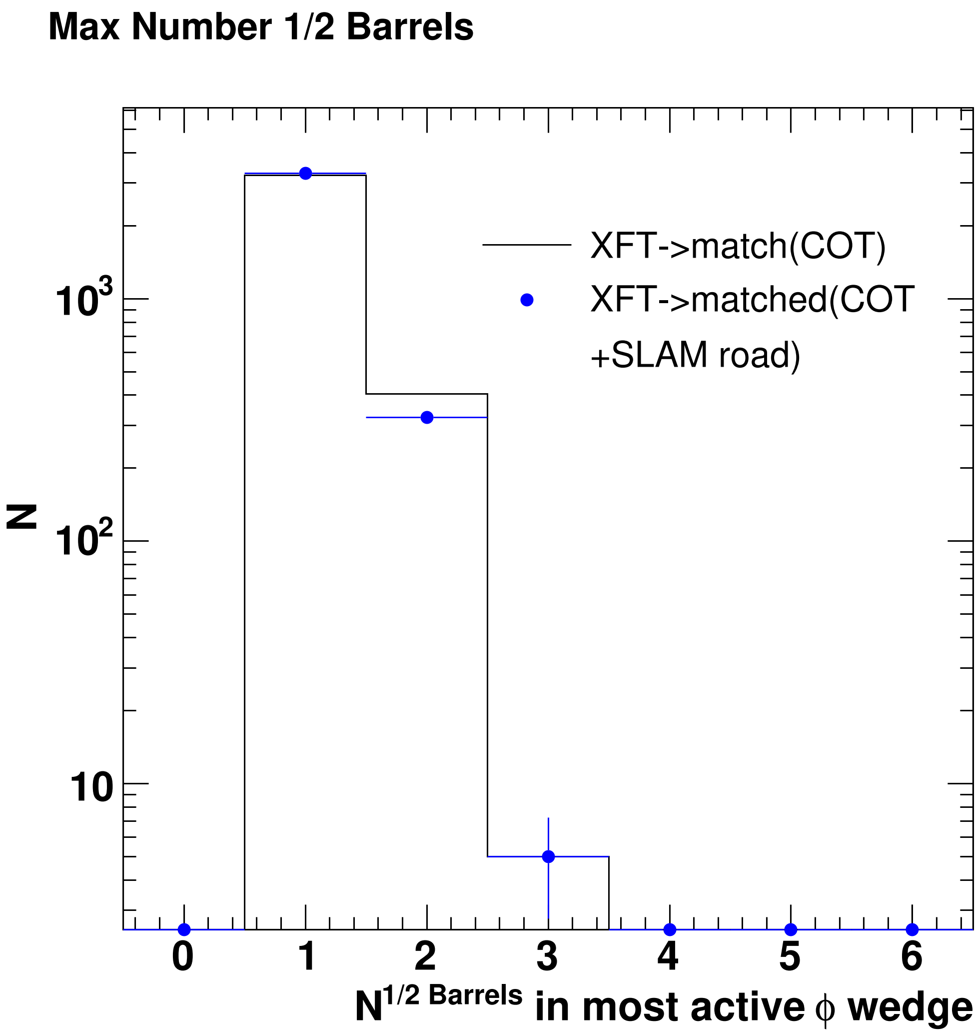

Figure 3: Maximum number of SVX-II half-barrels (determined by pointing the COT track to r_{Si3}) containing XFT tracks matched to COT tracks in the `blpc0d` data set.

4.2 Performance using SLAM output

In this case, each road identified by the SLAM module is used to set one of six bits that indicate whether a track extrapolates back to each of the six SVX-II half-barrels.

Gaussians are fitted the z_{Si3}^{SLAM} distributions for each of the SVX half-barrels (we ignore non-gaussian tails), a bit corresponding to a SVX half-barrel is set if z_{Si3}^{SLAM} is within $\pm n\sigma$ of the mean. The value of n is varied from 3 to 1 to see how much rejection is possible. In the $n = 1$ case, the mean is reduced from exactly 6 to ~ 5.5.

The fits that are used for setting bits are shown in figure 4 (usefull to note that a SVX half-barrel is ~ 14 cm long). The distribution of the maximum number of bits set in all 12 wedges is shown in Figure 5.

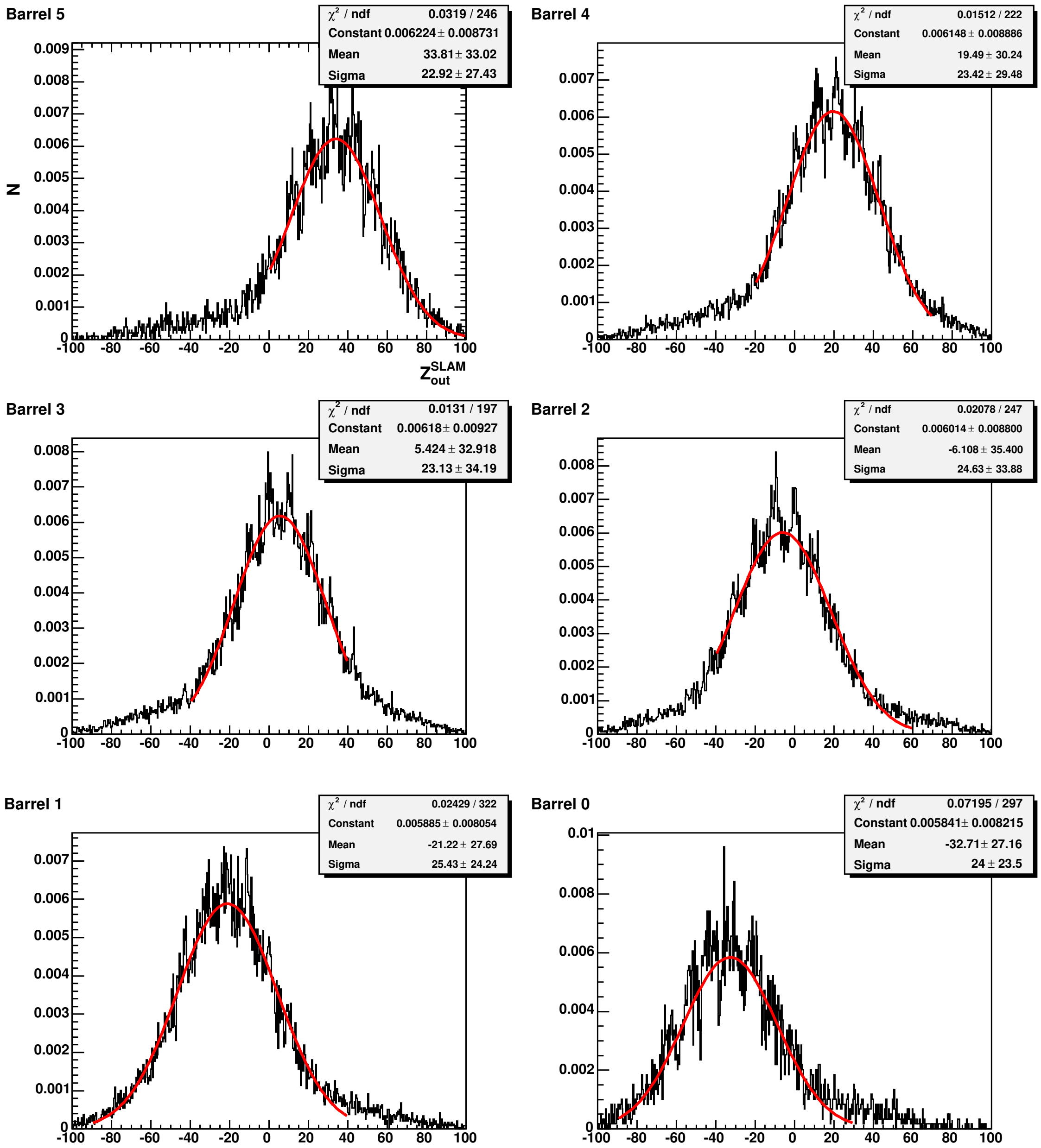

Figure 4: Gaussian fits to the z_{Si3}^{SLAM} distributions associated with the SVX half-barrels (`b1pc0d` data set), these fits are the input for the cuts used to set the 6 bits.

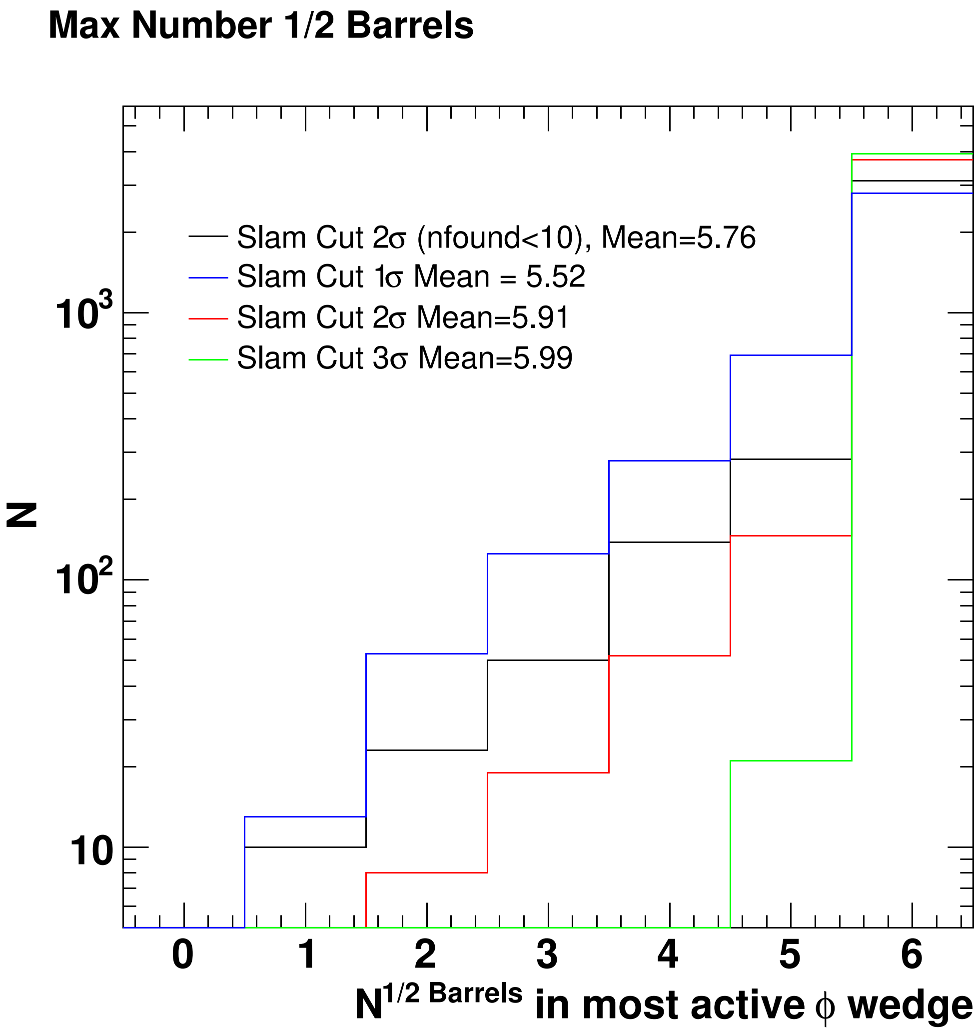

Figure 5: Maximum number of SVX-II half-barrels containing SLAM roads in the `blpc0d` data set.

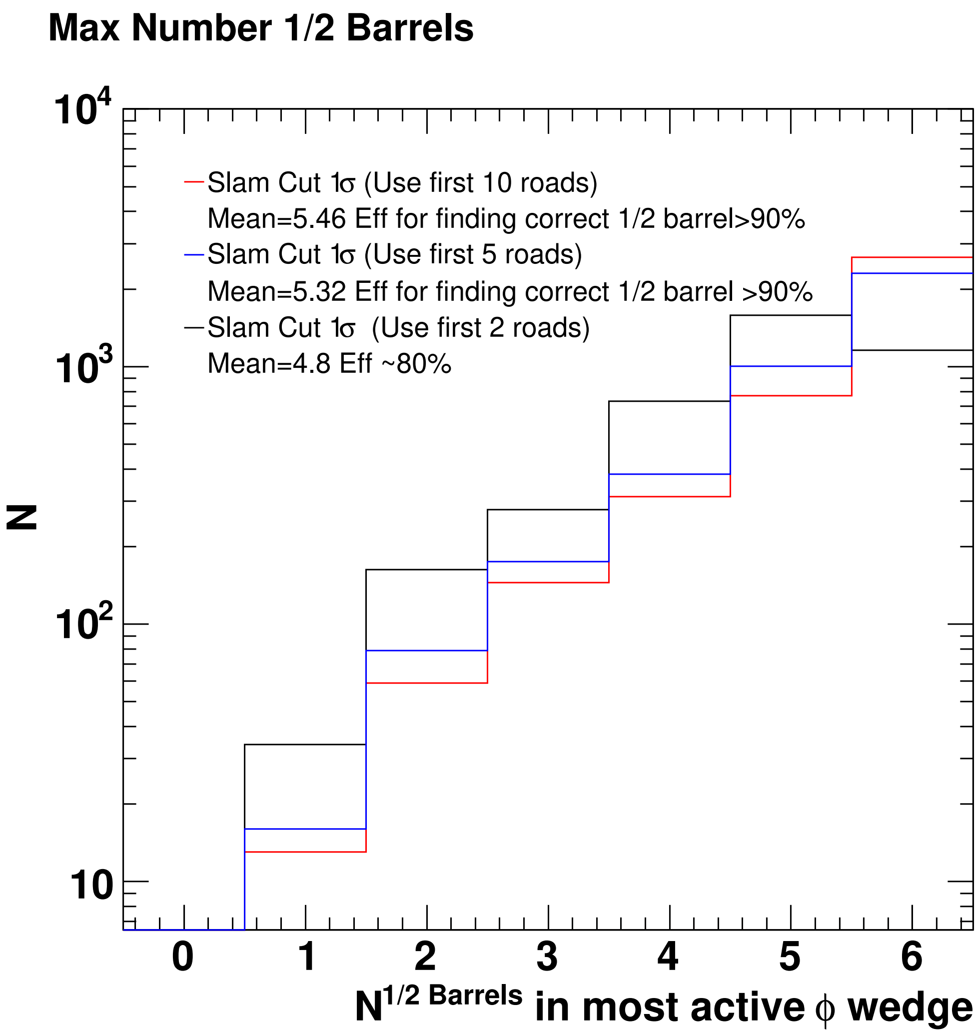

Figure 6: Maximum number of SVX-II half-barrels containing SLAM roads in the `blpc0d` data set. Only the first 10,5, and 2 roads are considered and the efficiency of finding the correct half barrel drops from $eff > 90\%$ for 10 and 5 roads to $\sim 80\%$ for 2 roads.

4.3 Faster track list at L2

Other benefits can be provided by the hardware that we propose to use for the barrel pointing algorithm. In particular, it will be possible to format a list of axial XFT tracks that have been confirmed by the SLAM modules and transmit it to the Level 2 SVT system in such a way that it arrives q clock cycles before the list provided by the current XTRP hardware. *What more to say...*

5 Performance Implications

Can we work out how much this will actually impact SVT processing time?

6 Properties of the SLAM output

The follow plots show some general characteristics of the SLAM output used in the previous section.

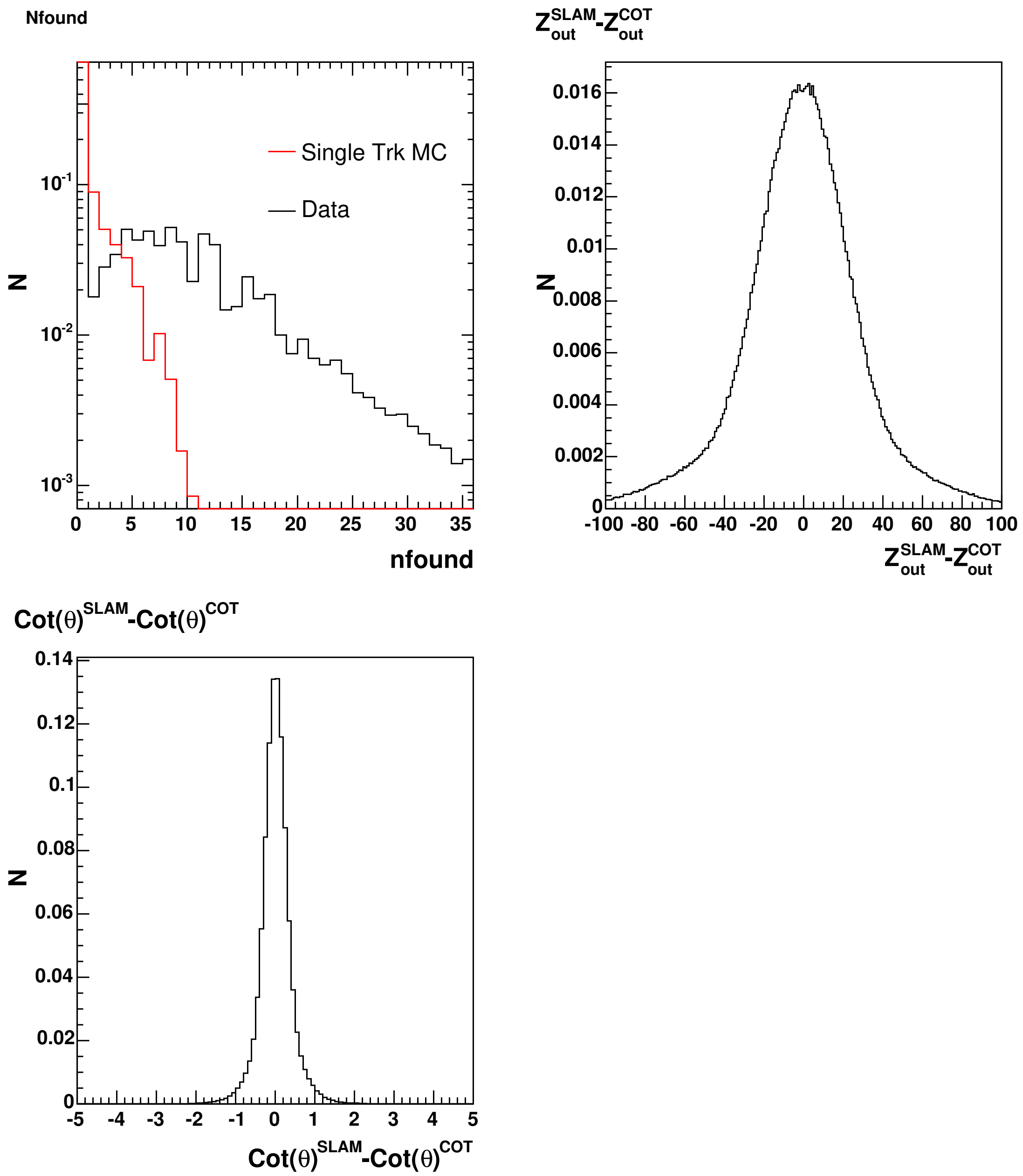

Figure 7: (a) Number of SLAM roads associated with XFT tracks in the `blpc0d` data set and single track MC, (b) $z_{Si3}^{SLAM} - z_{Si3}^{COT}$ for xft tracks matched to cot tracks and (c) $Cot(\theta)^{SLAM} - Cot(\theta)^{COT}$ for xft tracks matched to cot tracks.

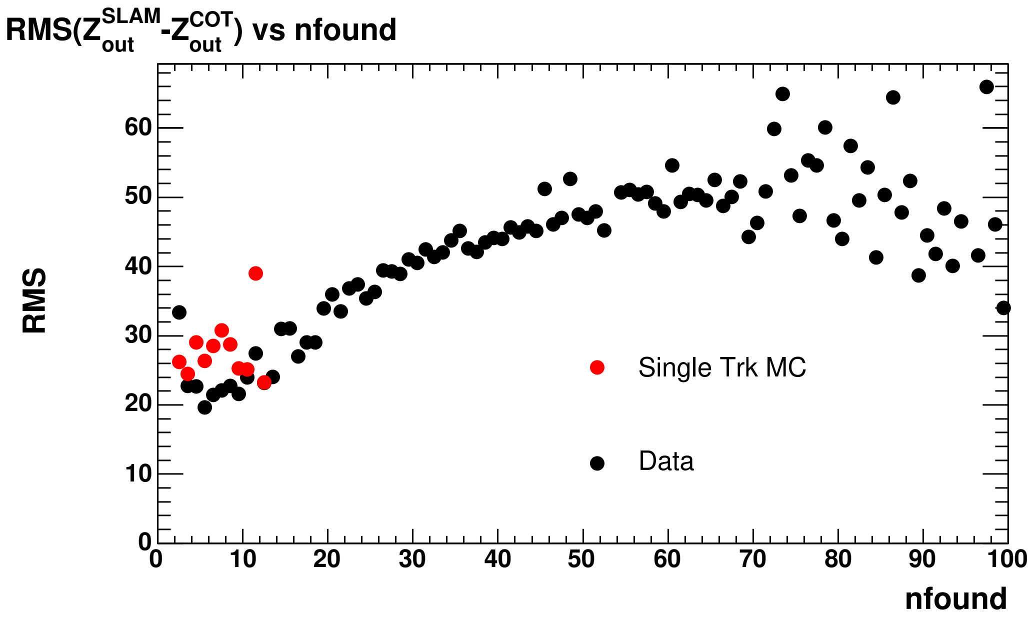

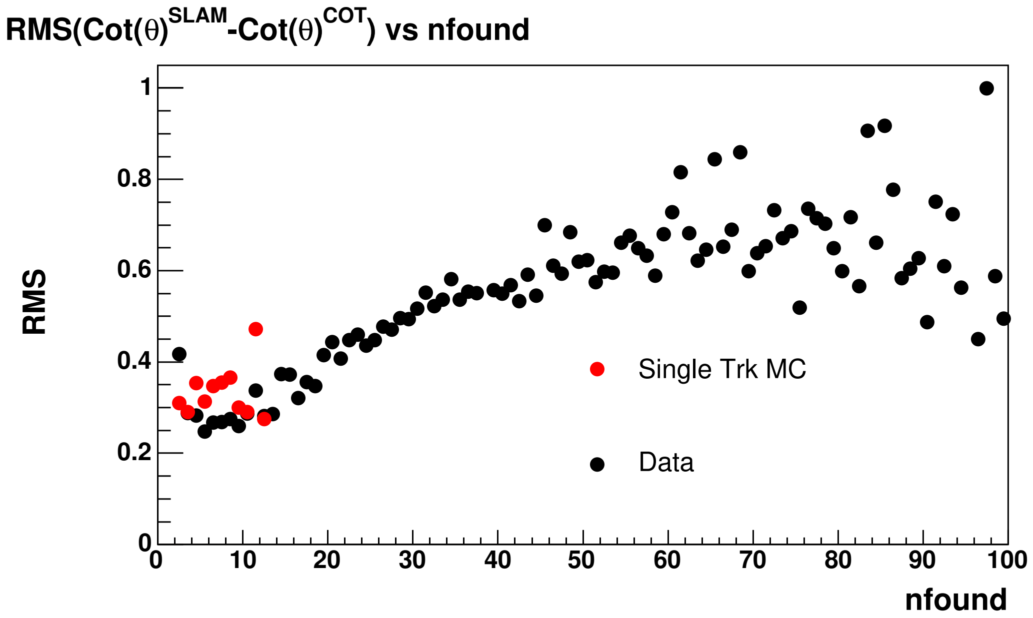

Figure 8: RMS of the $z_{Si3}^{SLAM} - z_{Si3}^{COT}$ and $Cot(\theta)^{SLAM} - Cot(\theta)^{COT}$ distributions as a function of the number of SLAM roads.

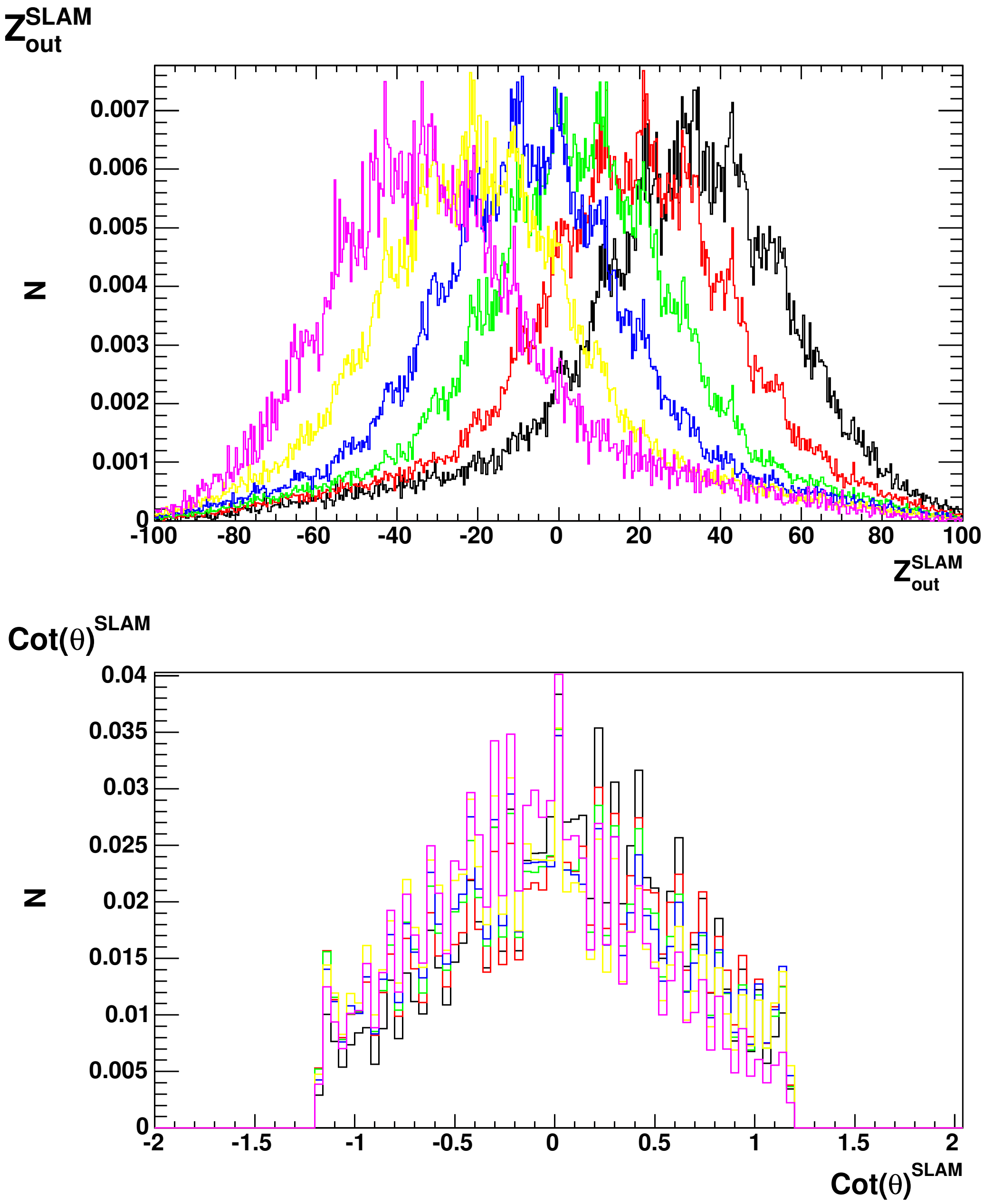

Figure 9: (a) For a given SVX half barrel (determined from COT track) the distributions of z_{Si3} form the SLAM roads associated with the XFT tracks originating from the half barrel and (b) same as a but $Cot(\theta)$

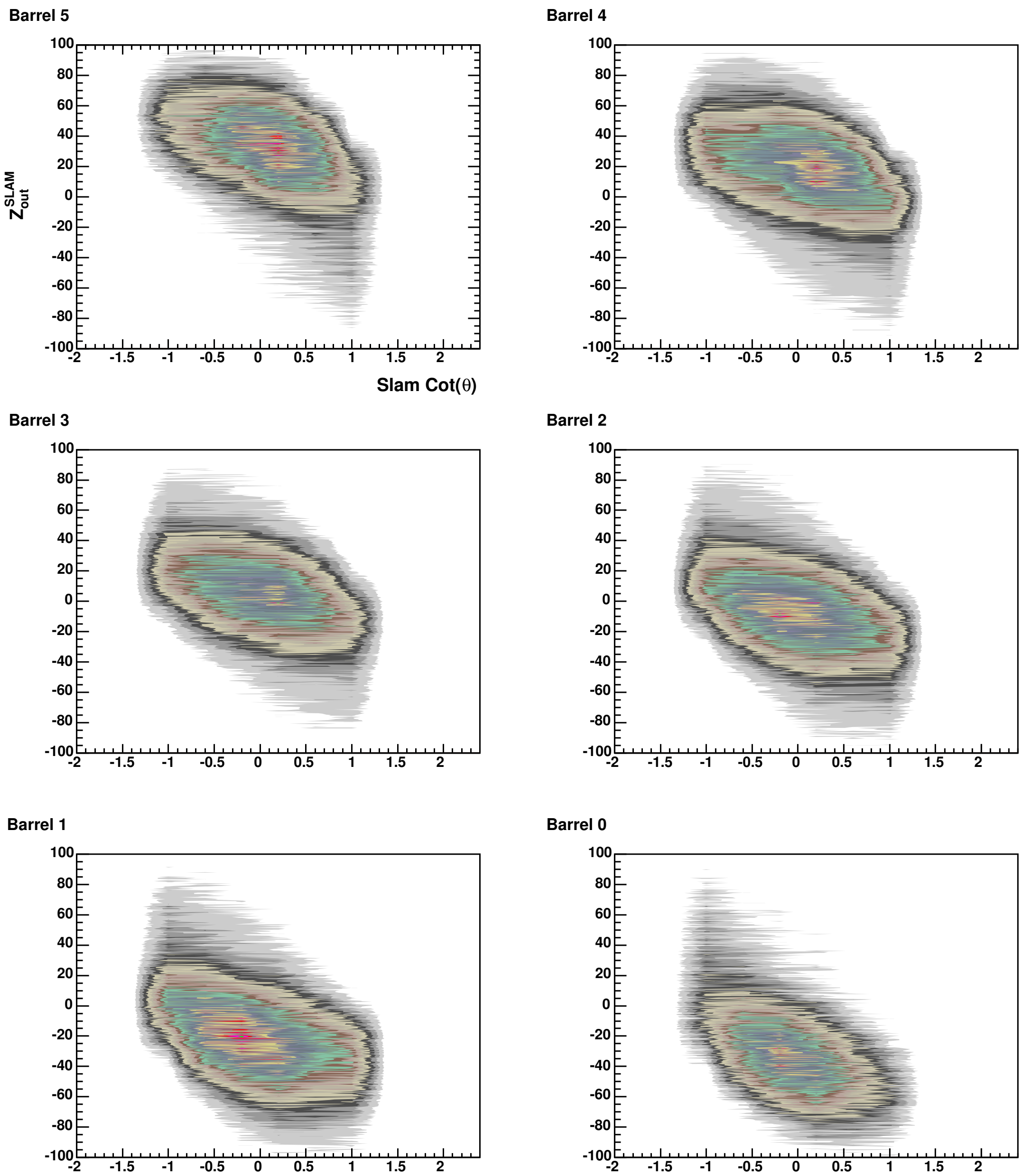

Figure 10: z_{Si3}^{SLAM} vs $Cot(\theta)^{SLAM}$ for the 6 SVX half barrels

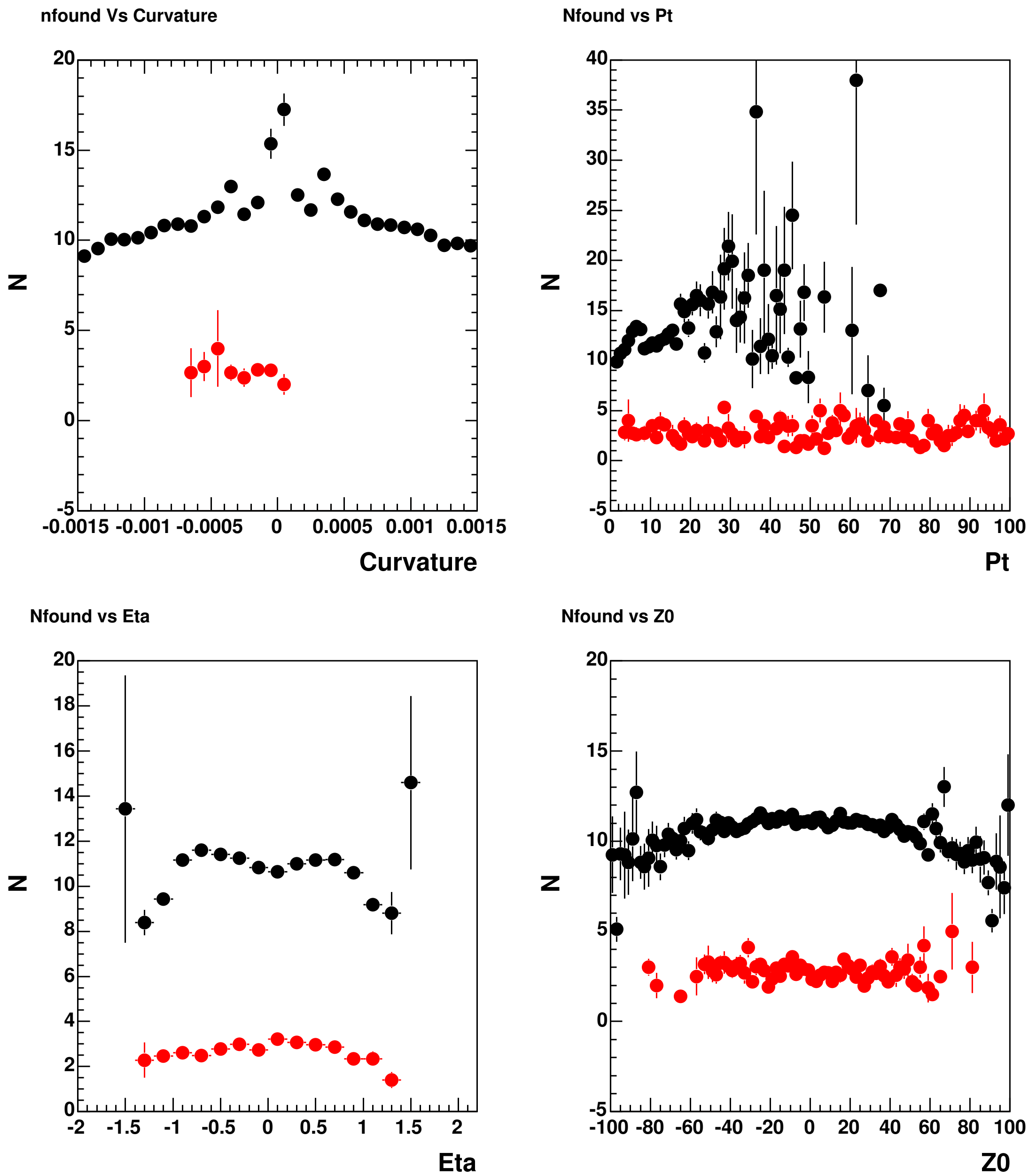

Figure 11: Number of SLAM roads found as a function of (a) curvature, (b) track P_T, (c) track η and (d) $z0$ in 1-trk Monte Carlo (red) and in the `blpc0d` dataset (black).

7 Conclusions

The number of half barrels that have tracks originating from them in the `blpc0d` dataset is typically much less than 6 at the luminosity studied. The mean for the half barrel distribution in the most active ϕ wedge is ~ 1.03 using the SVT half-barrel information.

Using cuts on the z_{Si3}^{SLAM} to point to a SVX half barrel provides a small reduction in the number of half-barrels found/(bits set) in the most active ϕ wedge. The mean of the distribution goes from exactly 6 to ~ 5.5 (for $\mu - 1\sigma \leq z_{Si3}^{SLAM} < \mu + 1\sigma$). The limited improvement is due to the resolution of the z_{Si3}^{SLAM}. The study is repeated using a subset of the slam roads (just loop over fewer than 10,5,2 etc not ranking by quality) to point to a SVX half barrel. This improves barrel rejection at the expense of the efficiency with which the correct SVX half-barrel is found.

References

[1] `http://cdfkits.fnal.gov/CdfCode/source/XFTSim/`

[2] R. Hughes, *et al.*, *The XFT SLAM Board Specification*, CDF Note 7073, June 23, 2004.

[3] H.-C. Fang, *et al.*, *SemiLeptonicB/LeptonSvtSel– An offline filter module for lepton-SVT data*, CDF Note 6326, February 13, 2003.

[4] J. Dittmann, *et al.*, *Run 2b XFT Stereo Mask Finding Specifications*, CDF Note 7789, August 22, 2005.